OX40 Agonist Therapy Enhances CD8 Infiltration and Decreases Immune Suppression in the Tumor

Michael J. Gough, Carl E. Ruby, William L. Redmond, Birat Dhungel, Alexis Brown, and Andrew D. Weinberg

Robert W. Franz Cancer Center, Earle A. Chiles Research Institute, Providence Portland Medical Center, Portland, Oregon

Abstract

Acquisition of full T-cell effector function and memory differentiation requires appropriate costimulatory signals, including ligation of the costimulatory molecule OX40 (TNFRSF4, CD134). Tumors often grow despite the presence of tumor-specific T cells and establish an environment with weak costimulation and immune suppression. Administration of OX40 agonists has been shown to significantly increase the survival of tumor-bearing mice and was dependent on the presence of both CD4 and CD8 T cells during tumor-specific priming. To understand how OX40 agonists work in mice with established tumors, we developed a model to study changes in immune cell populations within the tumor environment. We show here that systemic administration of OX40 agonist antibodies increased the proportion of CD8 T cells at the tumor site in three different tumor models. The function of the CD8 T cells at the tumor site was also increased by administration of OX40 agonist antibody, and we observed an increase in the proportion of antigen-specific CD8 T cells within the tumor. Despite decreases in the proportion of T regulatory cells at the tumor site, T regulatory cell function in the spleen was unaffected by OX40 agonist antibody therapy. Interestingly, administration of OX40 agonist antibody caused significant changes in the tumor stroma, including decreased macrophages, myeloid-derived suppressor cells, and decreased expression of transforming growth factor-β. Thus, therapies targeting OX40 dramatically changed the tumor environment by enhancing the infiltration and function of CD8 T cells combined with diminished suppressive influences within the tumor. [Cancer Res 2008;68(13):5206–15]

Introduction

The tumor necrosis factor receptor family member OX40 is expressed after activation of CD4 and CD8 T cells and has been shown to play critical roles in the differentiation and long-term survival of these cells (1–4). The ligand for OX40 (OX40L) can be found on antigen-presenting cells activated in the presence of strong adjuvant signals (5). T cells defective in expression of OX40 exhibited impaired generation of long-term memory when challenged with antigen in the presence of adjuvant (3, 6). In the absence of an adjuvant or danger signal, T-cell survival is extremely poor even in the presence of functional OX40 (1, 7). Provision of OX40 agonistic antibodies in the absence of a danger signal can replace the adjuvant effect, resulting in enhanced expansion of T cells and increased long-term memory T-cell populations (1). The majority of reports have identified important roles for OX40 in CD4 function (1–4), although agonistic antibodies to OX40 also have powerful effects on the proliferation, effector function, and long-term survival of CD8 T cells (8–11).

Growing tumors have been shown to serve as a continued source of antigen for T-cell priming in draining lymph nodes (12), and both circulating and tumor-infiltrating tumor antigen-specific T cells have been isolated from cancer patients (13, 14). Critical defects in these T cells, which prevent full effector function (15), can be overcome with *in vitro* restimulation (15) and *in vivo* vaccination (16). The development of long-term T-cell tolerance may be an important mechanism by which tumor cells evade immune surveillance. Whereas OX40L has been observed on antigen-presenting cells at sites of active autoimmune disease (17, 18), it has not been identified within the tumor environment. We and others have shown that systemic administration of agonistic antibodies to OX40 (αOX40) can replace the absence of OX40L within tumor-bearing hosts and leads to a significant increase in survival of tumor-bearing animals (19, 20).

T regulatory cells, defined by expression of FoxP3 and suppressive activity on naive T-cell proliferation, are of additional relevance in consideration of OX40 agonist therapy in established tumor models. The extent of T regulatory cell infiltration of tumor has been correlated with poor prognosis in cancer patients (21, 22). Depletion of T regulatory cells can significantly increase antitumor immune responses (23, 24), and inhibition of their function may have similar effects. Costimulation of TCR-stimulated T regulatory cells through CD28, GITR, or OX40 has been shown to inhibit their suppressive function (25–27). Therefore, αOX40 therapy may also inhibit the ability of T regulatory cells to suppress other T cells within the tumor environment.

For these reasons, we developed a model to examine the mechanism by which systemic αOX40 administration improves survival in mice with established tumors. In particular, we examined the role of tumor-infiltrating CD8 T cells, T regulatory cells and macrophages. We show here that a single administration of αOX40 to mice with established tumors resulted in a significant increase in CD8 T cells at the tumor site. Furthermore, these CD8 T cells were shown to exhibit increased effector function and an increased proportion of antigen-specific cells. Although we observed a significant decrease in the proportion of T regulatory cells in the tumor, the function of systemic T regulatory cells was not affected by *in vivo* administration of αOX40. We show that αOX40 induced changes in the tumor stroma; macrophages, myeloid-derived suppressors, and transforming growth factor-β (TGFβ) expression were all decreased. These changes suggest that administration of OX40 agonists to mice with established tumor

Note: Supplementary data for this article are available at Cancer Research Online (http://cancerres.aacrjournals.org/).

Requests for reprints: Andrew D. Weinberg, Robert W. Franz Cancer Center, Earle A. Chiles Research Institute, Providence Portland Medical Center, Portland, OR 97213. Phone: 503-215-2929; Fax: 503-215-6841; E-mail: andrew.weinberg@providence.org.

doi:10.1158/0008-5472.CAN-07-6484

can override tumor-induced deficiencies of CD8 T-cell function. Ultimately, these changes within the tumor may allow for improved immune function and improved tumor immunotherapy.

Materials and Methods

Animals, cell lines, and *in vivo* antibodies. C57BL/6 (6–8 wk old) mice were obtained from Charles River Laboratories for use in these experiments. OT1 mice, with CD8 T cells specific for the SIINFEKL epitope of ovalbumin, have previously been described (28). $OX40^{-/-}$ C57BL/6 mice (29) were kindly provided by Dr. N. Killeen (University of California San Francisco). $OX40^{-/-}$ OT1 mice were kindly provided by Dr. M. Croft (University of California San Diego). These experiments used the MCA205 H12 sarcoma, EMT6 mammary carcinoma, and CT26 colorectal carcinoma cell lines. Control RatIg antibody was purchased from Sigma, whereas rat anti-OX40 antibody (OX86), CD4-depleting antibody, and CD8-depleting antibody were produced in the laboratory from hybridomas and affinity purified over protein G columns. All animal protocols were approved by the institution's IACUC.

Tumor infiltrating cell harvest. C57BL/6 or BALB/c mice were injected s.c. on the right flank with 1×10^6 tumor cells, and tumors were allowed to develop a diameter of 5 to 7 mm. Mice were injected i.p. with 250 μg anti-OX40 or control RatIg, and tumors were monitored for 7 d. At day 7 after treatment, mice were sacrificed and the tumor was removed. The tumor was dissected into ~2 mm fragments followed by agitation in 1 mg/mL collagenase (Invitrogen), 100 μg/mL hyaluronidase (Sigma), and 20 mg/mL DNase (Sigma) in PBS for 1 to 2 h at room temperature. The digest was filtered through 100-μm nylon mesh to remove macroscopic debris, and the final cell preparation was separated by layering over Ficoll. Viable cells were counted and stained for flow cytometry. Control experiments established viable cell gating using 7AAD and confirmed that the cell preparation was >95% positive for the hematopoietic marker CD45.

Ovalbumin-expressing tumor cell lines. A lentiviral vector containing a transgene conferring surface-expressed ovalbumin was kindly provided by Dr. H-M. Hu of the Robert W. Franz Cancer Center in the Earle A. Chiles Research Institute. Tumor cell lines were infected with lentiviral vector at a multiplicity of infection of ~10:1 and went through two rounds of fluorescence-activated cell sorting (FACS) by surface staining with rabbit anti-ova (Sigma) followed by goat anti-rabbit PE (Jackson Immunoresearch). Sorted cultures were functionally assayed for the stable presence of ovalbumin by *in vitro* OT1 T-cell stimulation. To establish the more immunogenic MCA205 H12ova tumors, C57BL/6 mice had to be tolerized to ovalbumin via two i.v. injections of 500 μg ovalbumin (Sigma) 7 and 2 d before challenge with MCA205 H12ova.

Adoptive transfer. For adoptive transfer of naive OT1 cells, spleen and lymph nodes were harvested from $Thy1.1^+$ OT1 mice and the percentage of CD8 T cells was calculated by FACS analysis. 2.5×10^5 $CD8^+$ (OT1) cells were transferred i.v. into $Thy1.1^-Thy1.2^+$ tumor-bearing animals. OT1 $OX40^{-/-}$ mice did not bear the Thy1.1 congenic marker. Thus, in experiments involving these mice OT1 cells were identified by staining for CD8 along with the clonotypic Vα2 and Vβ5 TCR.

FACS antibodies and staining. Phenotyping of tumor-infiltrating cells was performed using the following antibodies: CD8 PETxRD (Caltag); CD8 PECy7, CD4 APC, CD4 PacificBlue, CD4 PECy7, CD11b FITC, CD62L FITC, CD62L APCCy7, CD25 APC, CD25 PE, Gr1 PE, Gr1 PECy7, IFNγ APC, TCRVα2 FITC (all Ebiosciences); TCRVβ5 PE (BD Biosciences); unlabeled Thy1.1 conjugated to PacificOrange in the laboratory using a PO-conjugation kit (Invitrogen); affinity-purified chicken anti-OX40 generated by Aves Labs., Inc.; and biotinylated (Pierce) for detection with streptavidin-PECy5 (Ebiosciences). Intracellular staining for FoxP3 was performed using an EBiosciences FoxP3 staining kit. For intracellular cytokine staining, 1×10^6 tumor-infiltrating cells were stimulated with 1 μg/mL anti-CD3 for 6 h at 37°C in the presence of Golgiplug (BD Biosciences). Cells were surface stained, fixed with 1% paraformaldehyde, and then intracellular staining was performed with an anticytokine antibody. Stained cells were analyzed on a BD FACSCalibur for four-color staining or BD LSRII for eight-color staining.

T regulatory cell functional assays. Mice were injected i.p. with 250 μg αOX40 or control RatIg, and spleens were harvested 7 d later. RBC were lysed, and splenocyte preparations were directly stained with CD4-FITC and CD25-PE. $CD4^+CD25^+$ cells were FACS sorted into >98% pure populations and seeded in triplicate at 5×10^4 per well in a 96-well round-bottomed plate. For purification of tumor macrophages, MCA205 H12 tumor-bearing mice were treated with 250 μg control RatIg or aOX40 i.p. and the tumor harvested after 7 d. Cell suspensions were prepared as above and stained with CD11b-FITC, Gr1-PE, and IA-PECy5. $CD11b^+Gr1^{hi}$ and $CD11b^+Gr1^{lo}$ cells were FACS sorted to >95% purity and seeded in triplicate at 5×10^4 per well. Responder CD8 cells were prepared from naive spleens by negative selection using a MACS CD8-negative selection kit (Miltenyi) and an AutoMACS cell sorter to 80% to 90% purity. $CD8^+$ cells were then CFSE labeled and washed thoroughly, and 5×10^4 per well were added to triplicate wells containing media (positive control), T regulatory cells, or macrophages. For preparation of accessory cells, splenocytes were stained with CD3-biotin (BD Biosciences), then washed, and bound with antibiotin beads (Miltenyi). $CD3^-$ accessory cells were negatively selected using an AutoMACS cell sorter to 95% to 98% purity, and 2×10^5 $CD3^-$ accessory cells were added to all wells. Cells were treated with 1 μg/mL anti-CD3 and harvested after 96 h. Harvested wells were stained for CD8 and CFSE dilution in CD8 responder cells calculated by flow cytometry.

Tumor-infiltrating cell RNA analysis. Tumor-infiltrating cells were prepared as above. For bulk analysis, total RNA was prepared from the mixed population using an RNeasy kit (Qiagen). T regulatory cells and macrophages were purified by FACS tumor-infiltrating lymphocytes (TIL) stained with CD4 PECy7 and CD25 PE or CD11b-FITC. Total RNA was prepared from the populations using an RNeasy kit (Qiagen). RNA (0.3 μg) was reverse transcribed into cDNA in a reaction containing 100 units MoMu LV reverse transcriptase (Invitrogen) in reaction buffer plus 5 mmol/L DTT, 500 mmol/L deoxynucleotide triphosphate, and 50 ng random hexamer primers. This reaction volume (1 μL) was used in a PCR reaction using HotStarTaq Plus Mix (Qiagen). Primer sequences were as follows: TGFβ 5′ CAAGGGCTACCATGCCAACTT, TGFβ 3′ ATGGGCAGTGGCTCCAAA (30); GAPDH 5′ TTAGCACCCCTGGCCAAGG, and GAPDH 3′ CTTACTCCTTGGAGGCCATG. For comprehensive analyses of tumor-infiltrating CD8 T-cell gene expression, tumor-infiltrating CD8+ cells were purified to >98% purity by FACS and total RNA was prepared as above. Microarray assays and data analysis were performed in the Affymetrix Microarray Core of the Oregon Health and Science University Gene Microarray Shared Resource.

Results

Influence of systemic αOX40 therapy on the tumor immune environment. To understand the mechanism by which αOX40 therapy caused immune-mediated rejection of established tumors, we examined the phenotype and function of immune cells isolated directly from tumors in three different models. The sarcoma cell line MCA205 H12 was injected s.c. into the flank of C57BL/6 mice, whereas the mammary carcinoma line EMT6 and the colorectal carcinoma CT26 were injected s.c. into the flank of BALB/c mice. Once the tumor reached 5 to 7 mm in diameter at ~10 to 14 d postinoculation, mice were treated with a single i.p. 250 μg dose of control RatIg or αOX40. At this time point, a single injection of aOX40 causes significant growth delay 7 d after treatment (Supplementary Fig. S1). Despite this effect, the αOX40 treated tumors resume growth resulting in no significant survival benefit of αOX40 treatment. To study the mechanism by which aOX40 influences tumor growth, 7 days after treatment, tumors were removed and subjected to triple-enzyme digest and tumor-infiltrating cells were isolated by density gradient centrifugation. Using multicolor flow cytometry, the phenotype of tumor-infiltrating immune cells was determined, applying the gating scheme shown in Fig. 1*A*.

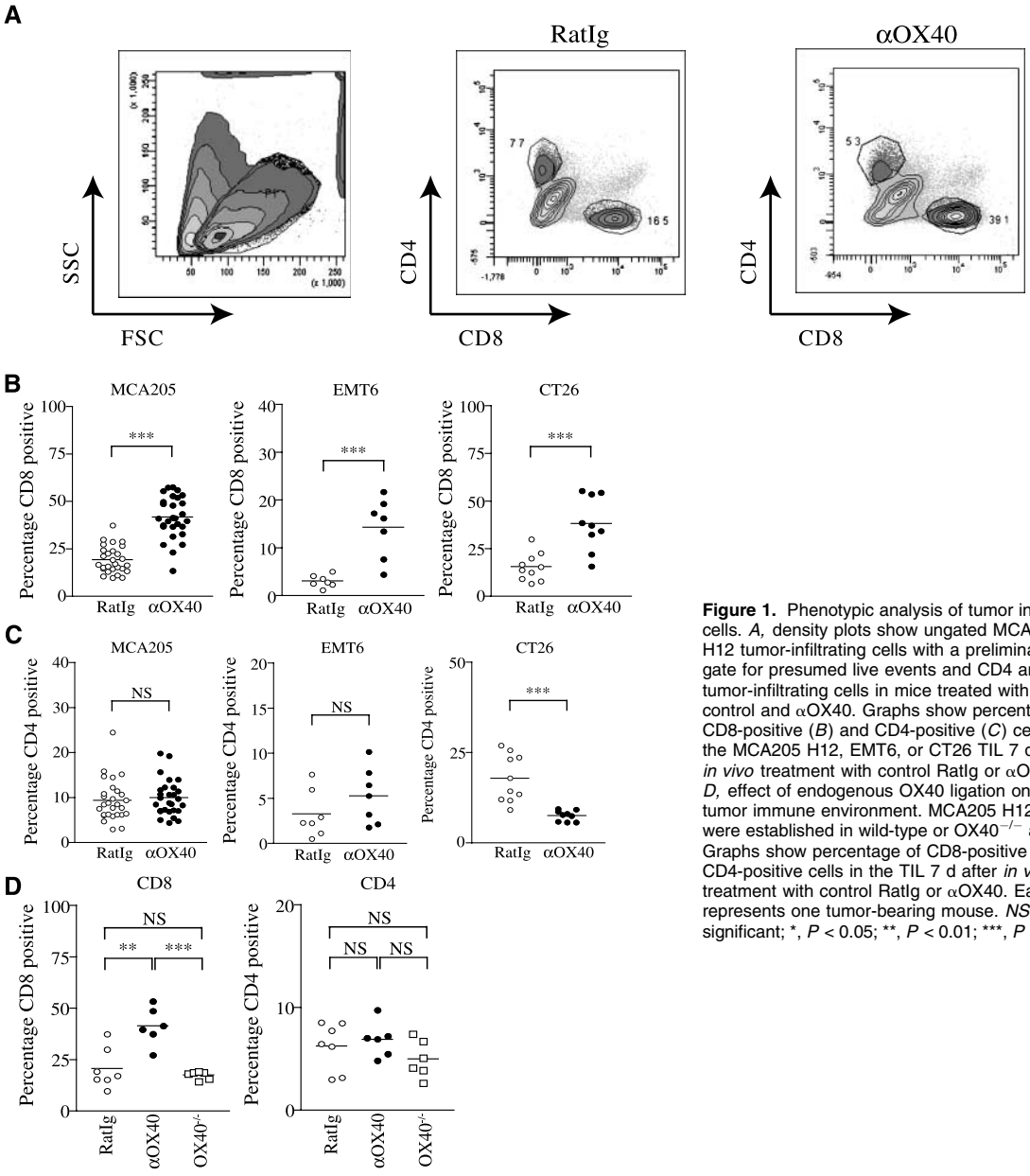

Figure 1. Phenotypic analysis of tumor infiltrating cells. *A,* density plots show ungated MCA205 H12 tumor-infiltrating cells with a preliminary gate for presumed live events and CD4 and CD8 tumor-infiltrating cells in mice treated with RatIg control and αOX40. Graphs show percentage of CD8-positive (*B*) and CD4-positive (*C*) cells in the MCA205 H12, EMT6, or CT26 TIL 7 d after *in vivo* treatment with control RatIg or αOX40. *D,* effect of endogenous OX40 ligation on the tumor immune environment. MCA205 H12 tumors were established in wild-type or $OX40^{-/-}$ animals. Graphs show percentage of CD8-positive and CD4-positive cells in the TIL 7 d after *in vivo* treatment with control RatIg or αOX40. Each icon represents one tumor-bearing mouse. *NS,* not significant; *, $P < 0.05$; **, $P < 0.01$; ***, $P < 0.001$.

We and others have previously shown that OX40 is expressed on recently activated CD4 and CD8 T cells, and αOX40 treatment leads to enhanced expansion and survival of antigen-activated CD4 and CD8 T cells (1–4, 8–11). After systemic αOX40 therapy, there was a dramatic increase in CD8 T cells at the tumor site in the MCA205 sarcoma, EMT6 breast carcinoma and CT26 colorectal carcinoma models (Fig. 1*B*). These changes were statistically significant and represented a 2-fold (19.38 ± 1.335:41.79 ± 2.098), 4.5-fold (3.104 ± 0.4836:14.29 ± 2.363), and 2.5-fold (15.55 ± 2.285:38.26 ± 4.730) change in CD8 proportion in the tumor site for the MCA205, EMT6, and CT26 tumor models, respectively. It is notable that the most immunogenic tumor, EMT6, exhibited the greatest CD8 response to OX40 therapy. The change in percentage of CD8 T cells also represented a significant increase in the number of $CD8/mm^3$ of tumor (10,480 ± 1,746:21,280 ± 4,275; Supplementary Fig. S1). Interestingly, systemic αOX40 therapy did not increase the proportion of CD4 T cells at the tumor site; the proportion present in CT26 tumors actually decreased (Fig. 1*C*). Because untreated tumors have a CD8 infiltrate, we sought to determine if endogenous OX40-OX40L interactions were necessary for development of the endogenous CD8 tumor infiltrate. There was no significant difference in the tumor CD8 infiltrate in untreated wild-type mice compared with $OX40^{-/-}$ mice (Fig. 1*D*). These data suggest that the growing tumor environment does not provide OX40-specific signals and supports the rationale for administration of OX40 agonists to tumor-bearing animals.

To understand whether the increase in infiltrating CD8 T cells brought about by systemic αOX40 therapy represent a simple increase in number or a functionally distinct population, we further characterized these cells. To assess their function, the

tumor-infiltrating cells were stimulated *in vitro* with αCD3 in the presence of secretion inhibitors and then stained for intracellular IFNγ. The tumor-infiltrating CD8 cells from all mice treated with control RatIg were relatively unresponsive; few cells produced IFNγ upon αCD3 stimulation (Fig. 2*A*). However, αOX40 significantly increased tumor-infiltrating CD8 T-cell production of IFNγ upon αCD3 stimulation in the sarcoma, breast carcinoma, and colorectal carcinoma models (Fig. 2*A*). These data suggest that the CD8 T cells within the tumor environment are functionally different after administration of αOX40. Of the many surface markers analyzed, only CD62L showed a significant change in expression (Fig. 2*B*). These data were confirmed by obtaining highly purified CD8 T cells from the tumor site by sorting and preparing RNA for microarray analysis. CD62L mRNA was down-regulated in the tumor-infiltrating CD8 T cells (MCA205 4.29-fold, CT26 1.32-fold). Infiltrating cells also showed decreased CCR7 expression (MCA205 3.03-fold, CT26 1.41-fold), which along with decreased CD62L suggests that tumor-infiltrating T cells tend to have an effector phenotype. Simultaneously, increases in CCR5 (MCA205 1.62-fold, CT26 1.41-fold) and CXCR6 (MCA205 1.52-fold, CT26 4.59-fold) mRNA were observed. Each of the phenotypes are suggestive of peripheral effector T cells trafficking to inflammatory sites (31–33) and suggest that systemic αOX40 therapy resulted in a qualitative change in the CD8 T cells and enabled them to infiltrate the tumor site.

To identify whether this αOX40-induced increase in tumor-infiltrating CD8 T cells was due to recruitment of tumor antigen-specific T cells, we engineered MCA205 H12 cells to express the model antigen ovalbumin and tracked ovalbumin-specific OT1 cells *in vivo*. MCA205 H12ova tumors were established in Thy1.2$^+$ mice that had been previously tolerized to ovalbumin. Naive OT1 Thy1.1$^+$ splenocytes were adoptively transferred to tumor-bearing mice that were treated with a single 250-μg dose of either control RatIg or αOX40. Treatment with αOX40 significantly increased the proportion of tumor-infiltrating Thy1.1$^+$ OT1 T cells (Fig. 2*C*). To determine whether the increase in CD8 T cells at the tumor site was the result of direct OX40 stimulation on CD8 cells or was indirect via stimulation of other OX40-expressing populations, we examined the effects of αOX40 stimulation where the antigen-specific CD8 T cells were deficient in OX40 expression. Naive wild-type or OX40$^{-/-}$ OT1 splenocytes were adoptively transferred to mice bearing established MCA205 H12ova tumors. Mice were then treated with a single 250-μg dose of control RatIg or αOX40. αOX40 treatment resulted in a significant increase in tumor-infiltrating Vα2$^+$Vβ5$^+$ OT1 cells, but only when the adoptively transferred CD8 T cells expressed OX40 (Fig. 2*D*). In these transfer experiments, the endogenous CD8 T-cell response within the tumor stimulated via αOX40 treatment was still intact (data not shown). These data strongly suggest that OX40 expression on the antigen-specific CD8 T cells is required for the αOX40-mediated increase in CD8 T cells within the tumor environment.

To understand the mechanisms by which antigen-specific T cells accumulate in the tumors of treated animals, we adoptively transferred CFSE-labeled OT1 cells to tumor-bearing mice and analyzed the tumor, draining lymph node and nondraining lymph node over a time course. OT1 were first seen to expand in the draining lymph node, after which the cells accumulate at the tumor site (Supplementary Fig. S2). No expansion or accumulation is observed in the nondraining lymph node (Supplementary Fig. S2). Examining the CFSE profile of the OT1 cells shows a steady dilution of CFSE over time, indicative of rapid and continued division (Supplementary Fig. S2). Interestingly, whereas the

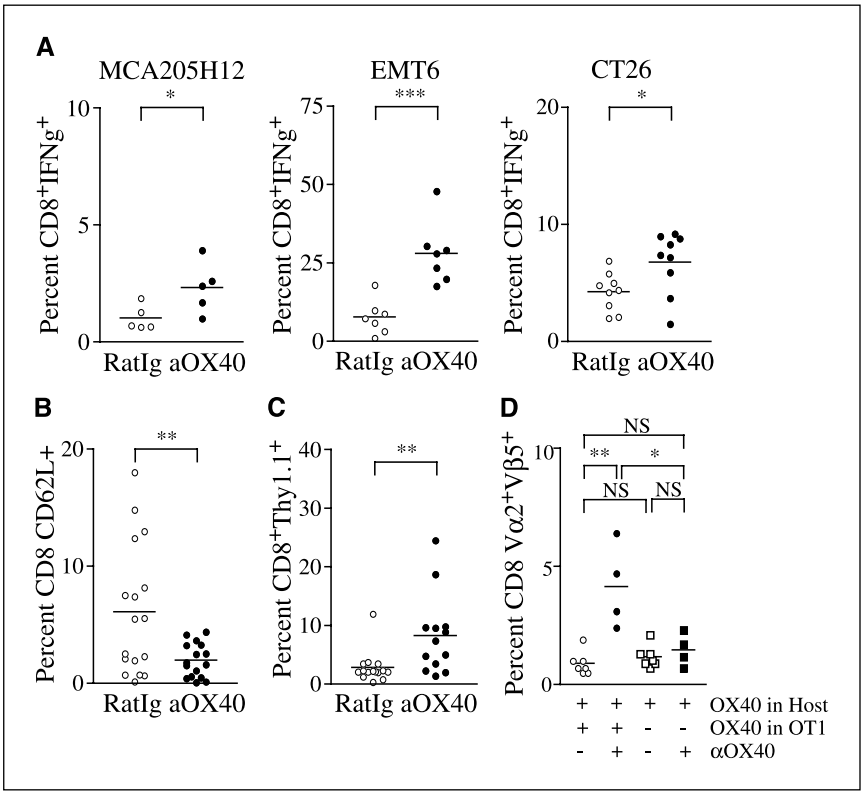

Figure 2. Functional analysis of tumor-infiltrating CD8 T cells. *A,* tumor-infiltrating cells from MCA205 H12, EMT6, or CT26 were isolated 7 d after *in vivo* treatment with control RatIg or αOX40, stimulated *in vitro* with αCD3 for 5 to 6 h in the presence of secretion inhibitors, and analyzed for IFNγ expression in CD8$^+$ cells. *B,* CD62L expression on CD8$^+$ T cells infiltrating the tumor 7 d after *in vivo* treatment with control RatIg or αOX40. *C,* antigen-specific T-cell accumulation at the tumor site. Mice bearing MCA205ova tumors were given 2.5 × 10^5 Thy1.1$^+$OT1 cells i.v., and treated with control RatIg or αOX40. At 7 d later, tumor-infiltrating cells were harvested and analyzed for the percentage of CD8$^+$ cells that were Thy1.1$^+$ OT1 cells. *D,* importance of OX40 expression on the ability of antigen-specific CD8 cells to infiltrate the tumors after systemic αOX40 therapy. MCA205 H12ova tumors were established in wild-type mice, given 2.5 × 10^5 OT1 or OX40$^{-/-}$OT1 cells i.v., and treated with control RatIg or αOX40. At 7 d after αOX40 treatment, tumor-infiltrating cells were harvested and analyzed for the percentage of tumor-infiltrating CD8$^+$ cells that were Vα2$^+$Vβ5$^+$ OT1 cells. Each icon represents one tumor-bearing mouse. *, $P < 0.05$; **, $P < 0.01$; ***, $P < 0.001$.

draining lymph node contains cells in a range of divisions, the tumor contains only the leading edge of cell division. These data support the hypothesis that the tumor-infiltrating CD8 T cells are exclusively effector-phenotype cells that are generated in the draining lymph node then traffic to the peripheral tumor site.

Role of T regulatory cells in systemic αOX40 therapy. Growing tumors reportedly attract a large population of T regulatory cells that express OX40, and treatment with αOX40 has been shown to suppress inducible T regulatory cell development and function *in vitro* (25–27). Thus, it is possible that systemic administration of αOX40 suppresses T regulatory cells resulting in enhanced CD8 T-cell effector function *in vivo*. Intracellular staining for FoxP3 showed that a large proportion of $CD4^+$ cells within the tumor coexpress CD25 and FoxP3 (Fig. 3*A*). These $CD4^+CD25^+FoxP3^+$ T regulatory cells were also $OX40^+$, which was confirmed by analyzing tumors grown in $OX40^{-/-}$ animals (Fig. 3*A*). The population of $CD4^+$ cells that were $CD25^+FoxP3^+$ T regulatory cells in the tumor was significantly decreased after αOX40 treatment in MCA205 H12 and EMT6 tumors, but not in the CT26 tumors (Fig. 3*B*). However, in the MCA205 H12 tumor, this small change in percentage of T regulatory cells did not represent a significant change when analyzed as the number of

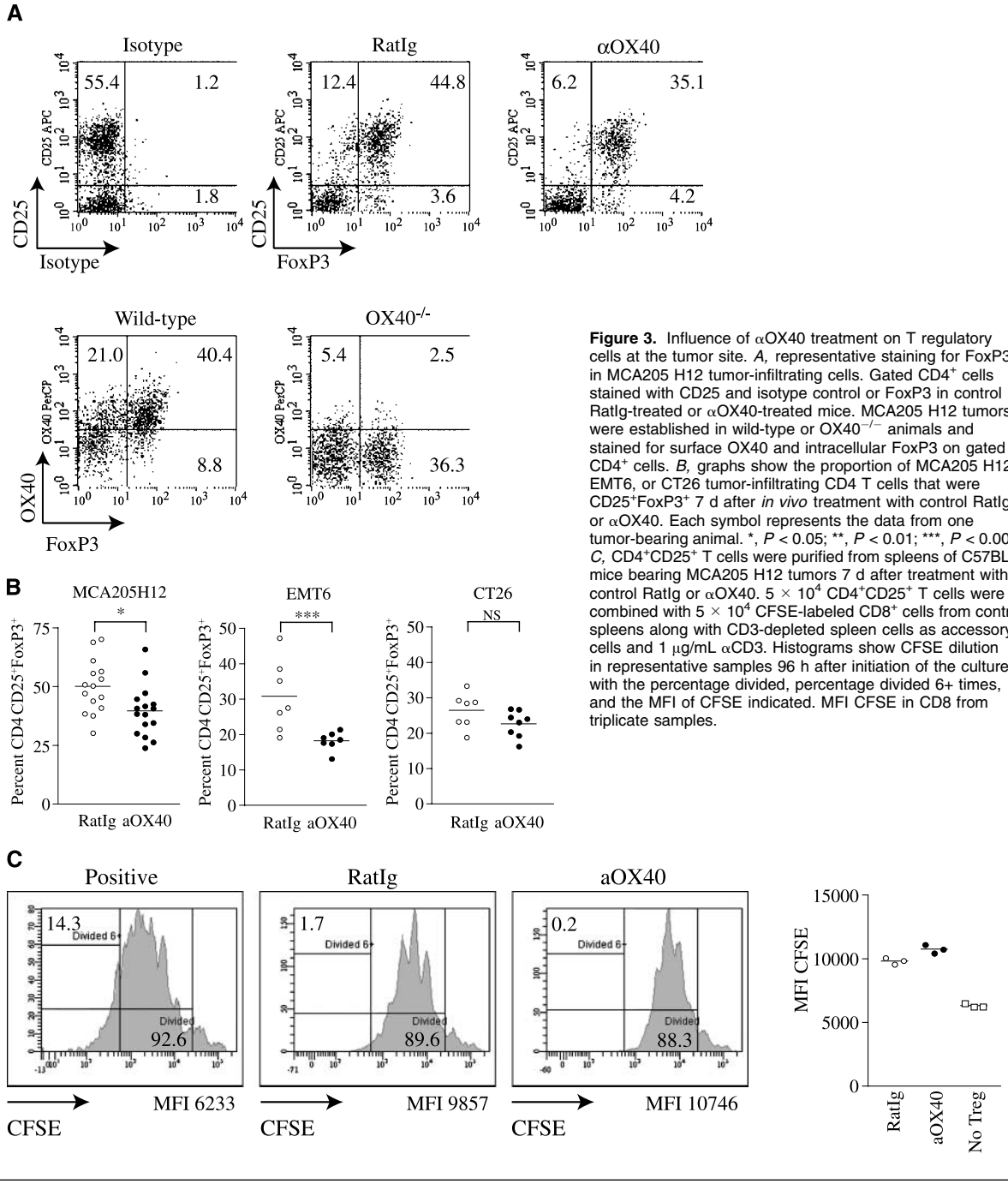

Figure 3. Influence of αOX40 treatment on T regulatory cells at the tumor site. *A,* representative staining for FoxP3 in MCA205 H12 tumor-infiltrating cells. Gated $CD4^+$ cells stained with CD25 and isotype control or FoxP3 in control RatIg-treated or αOX40-treated mice. MCA205 H12 tumors were established in wild-type or $OX40^{-/-}$ animals and stained for surface OX40 and intracellular FoxP3 on gated $CD4^+$ cells. *B,* graphs show the proportion of MCA205 H12, EMT6, or CT26 tumor-infiltrating CD4 T cells that were $CD25^+FoxP3^+$ 7 d after *in vivo* treatment with control RatIg or αOX40. Each symbol represents the data from one tumor-bearing animal. *, $P < 0.05$; **, $P < 0.01$; ***, $P < 0.001$. *C,* $CD4^+CD25^+$ T cells were purified from spleens of C57BL/6 mice bearing MCA205 H12 tumors 7 d after treatment with control RatIg or αOX40. 5×10^4 $CD4^+CD25^+$ T cells were combined with 5×10^4 CFSE-labeled $CD8^+$ cells from control spleens along with CD3-depleted spleen cells as accessory cells and 1 μg/mL αCD3. Histograms show CFSE dilution in representative samples 96 h after initiation of the culture, with the percentage divided, percentage divided 6+ times, and the MFI of CFSE indicated. MFI CFSE in CD8 from triplicate samples.

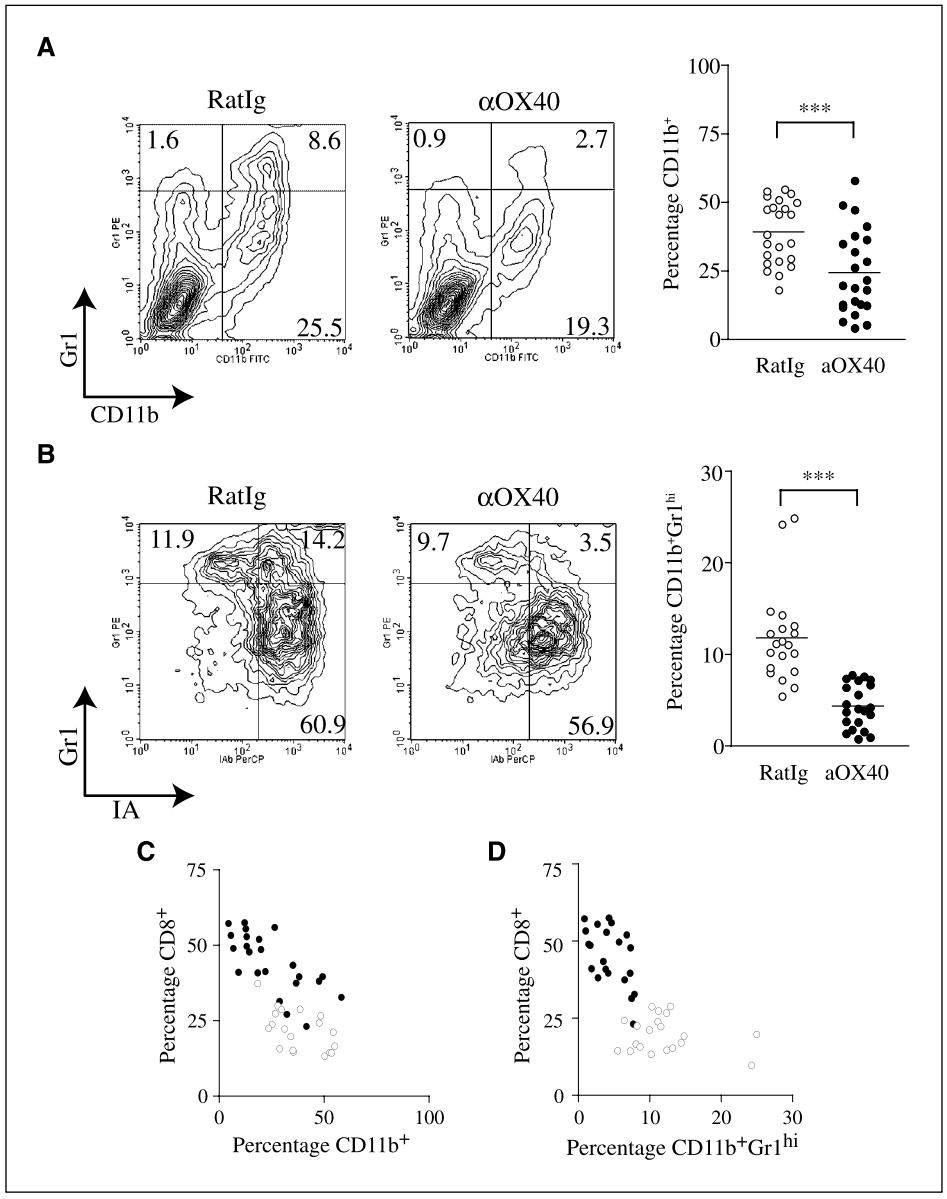

Figure 4. Influence of αOX40 treatment on accumulation and maturation of macrophages at the tumor site. *A,* phenotypic analysis of tumor infiltrates 7 d after *in vivo* treatment with control RatIg or αOX40. Representative contour plots from control RatIg-treated and αOX40-treated tumors, and the effect of αOX40-treatment on the proportion of $CD11b^+$ cells. *B,* gating on $CD11b^+$ cells, representative contour plots show expression of Gr1 and IA in control RatIg-treated and αOX40-treated tumors and the effect of αOX40-treatment on the proportion of $CD11b^+Gr1^{hi}$ cells. *C* and *D,* the data from multiple control (*open circle*) and αOX40 (*filled circle*)–treated animals showing within each tumor the percentage of tumor infiltrating cells that are CD8-positive compared with $CD11b^+$ (*C*) and $CD11b^+Gr1^{hi}$ (*D*). Each symbol represents the data from one tumor-bearing animal. *, $P < 0.05$; **, $P < 0.01$; ***, $P < 0.001$.

$CD4^+CD25^+FoxP3^+/mm^3$ of tumor (3,348 ± 1,376:2,292 ± 469; Supplementary Fig. S1). In view of the increase in CD8 T cells described in Fig. 1, it is notable that the ratio of CD8 T cells to T regulatory cells within the tumor was dramatically altered by αOX40 in each model, from 6.2:1 (±1.615) to 13.3:1 (±1.736) for MCA205, 4.2:1 (±0.3824) to 21.7:1 (±6.882) for EMT6, and 5.2:1 (±0.5814) to 22.1:1 (±3.774) for CT26. To determine whether αOX40 therapy decreased systemic T regulatory cell function *in vivo*, we purified $CD4^+CD25^+$ cells isolated from the spleens of mice 7 days after control RatIg or αOX40. CD8 T-cell proliferation was similarly inhibited by addition of $CD4^+CD25^+$ cells from control mice or αOX40-treated mice (Fig. 3*C*).

Influence of αOX40 therapy on macrophages within the tumor immune environment. Macrophages are a major cell population in tumors and have been associated with both protumor and antitumor activity. Staining MCA205 H12 tumors for CD11b identified a large population of infiltrating macrophages (Fig. 4*A*), which significantly decreased after systemic αOX40 treatment. The $CD11b^+$ population within the tumor could be further subclassified by expression of the immature myeloid marker Gr1 and MHC class II into two distinct populations (Fig. 4*B*). The immature $CD11b^+Gr1^{hi}$ cell population is phenotypically consistent with the myeloid-derived suppressor cell population (MDSC) that has been reported to inhibit T cell–mediated immune responses *in vitro* and *in vivo* (34, 35). Interestingly, systemic administration of αOX40 significantly decreased this $CD11b^+Gr1^{hi}$ cell population in the tumor site (Fig. 4*B*). The frequency of both $CD11b^+$ and $CD11b^+Gr1^{hi}$ was inversely correlated with the percentage of CD8 T cells at the tumor site (Fig. 4*C* and *D*). Thus, αOX40 treatment significantly elevated the ratios of CD8 T cells to $CD11b^+$ and $CD11b^+Gr1^{hi}$ cells at the tumor site from 0.6:1 (±0.08725) to 3.3:1 (±0.6776) and 1.9:1 (±0.1797) to 17.8:1 (±3.923), respectively. The change in percentage of $CD11b^+$ and $CD11b^+Gr1^{hi}$ cells also represented a significant decrease in the number of these cells per cubic millimeter of tumor ($CD11b^+$ 23,230 ± 3,565:12,320 ± 2,529; $CD11b^+Gr1^{hi}$ 5,426 ± 1,171:1,919 ± 405.8; Supplementary Fig. S1).

MDSC share some phenotypic features with neutrophils, which have been shown to express OX40 and respond to OX40 ligation. We have been unable to detect the presence of OX40 on MDSC at the tumor site, suggesting that these are secondary effects of OX40 ligation on CD4 or CD8 T cells. To address this question, we analyzed the effect of depleting lymphocyte populations on tumor macrophages. We still observed a significant decrease in $CD11b^+Gr1^{hi}$ cells in CD4-depleted mice given αOX40 (Fig. 5*A*). Depletion of endogenous CD8 cells significantly increased the proportion of immature $CD11b^+Gr1^{hi}$ cells in the tumor (Fig. 5*A*). In the absence of CD8 T cells, the proportion of $CD11b^+Gr1^{hi}$ cells remained high even after αOX40 treatment (Fig. 5*A*). Thus, it seems that CD8 T cells infiltrating the tumor influence the attraction and/or differentiation of tumor-associated macrophage populations.

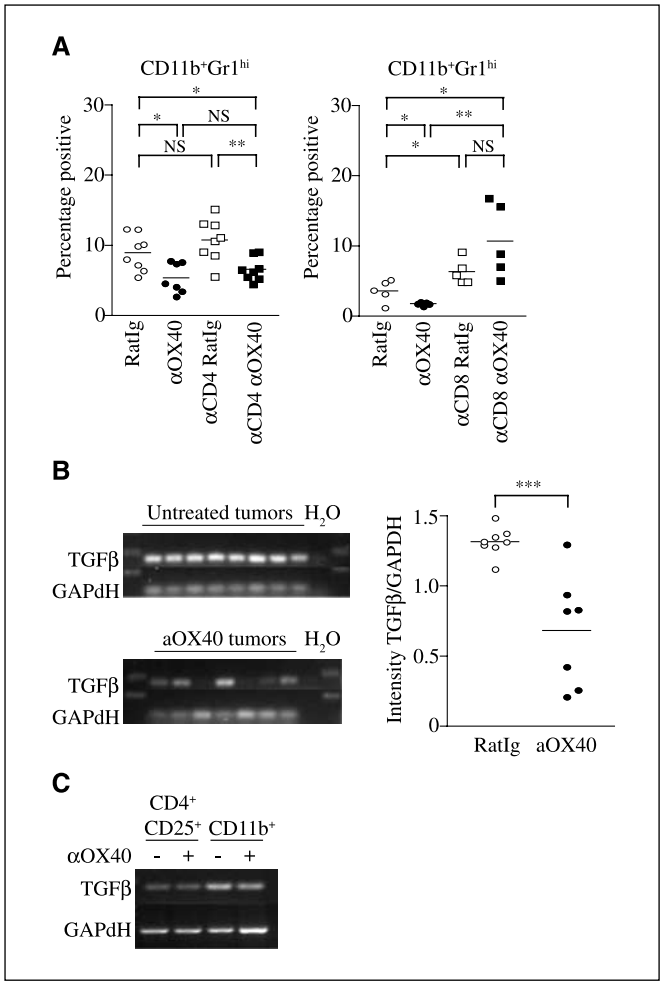

Figure 5. Importance of CD4 and CD8 T cells in the establishment of the macrophage phenotype and the effect of αOX40. *A,* mice with established MCA205 H12 tumors were left untreated or treated with CD4-depleting antibodies or CD8-depleting antibodies 2 d before and 5 d after RatIg or αOX40 treatment. Phenotypic analysis of tumor infiltrating cells was performed on day 7. Graphs show the percentage of tumor-infiltrating cells that were $CD11b^+Gr1^{hi}$. *B,* tumor environment changes after αOX40 treatment. RNA was purified from total tumor-infiltrating cells, then RT-PCR was performed using primers specific for *tgfb1*or GAPDH. The gel image from the *tgfb1*PCR has been digitally positioned over the matching GAPDH PCR. Each lane represents the results from one RatIg control or αOX40-treated tumor. The graph shows quantitation of PCR band intensities to determine relative intensity of TGFβ/GAPDH. Each symbol represents the data from one tumor-bearing animal. *, $P < 0.05$; **, $P < 0.01$; ***, $P < 0.001$. *C,* RNA was purified from FACS sorted tumor infiltrating $CD11b^+$ and $CD4^+CD25^+$ populations 7 d after *in vivo* treatment with control RatIg or αOX40, and RT-PCR was performed using primers specific for *tgfb1* or GAPDH.

Inhibitory molecule expression in the tumor immune environment. We hypothesized that the changes in T regulatory cells, macrophages, and CD8 T cells would further alter the tumor environment. TGFβ is an important cytokine in the generation and function of both T regulatory cells and MDSC (36, 37), and inhibition of TGFβ effects on CD8 T cells has been shown to enhance CD8 infiltration and effector function at the tumor site (38). To determine whether αOX40 altered TGFβ expression at the tumor site, we isolated RNA from tumor infiltrating cells and performed reverse transcription–PCR (RT-PCR) for TGFβ and the housekeeping gene GAPDH (Fig. 5*B*). TGFβ was expressed by the tumor-infiltrating cells from control RatIg-treated mice and was less detectable in αOX40-treated mice. Densitometry of the gels from Fig. 5*C* showed a significant decrease in the intensity of the TGFβ signal in tumor-infiltrating cells from αOX40-treated mice (Fig. 5*B*). Because TGFβ expression has been described in both T-regulatory cells and suppressive macrophages (36, 37), we purified $CD4^+CD25^+$ and $CD11b^+$ cells from tumor-infiltrating cells by cell sorting. RT-PCR showed that both T regulatory cells and macrophages expressed TGFβ RNA and the TGFβ signal was not greatly altered in T regulatory cells or macrophages by systemic αOX40 therapy (Fig. 5*C*). These data suggest that the decrease in TGFβ RT-PCR signal in cells from tumors after αOX40 therapy may be due to the decrease in number of TGFβ-expressing cells (T regulatory cell and macrophage populations; Figs. 3 and 4), rather than reduced expression by individual cells.

Inhibition of CD8 T-cell responses by macrophages. A further mechanism by which macrophages have been shown to inhibit T-cell responses is through expression of arginase (39). The presence of arginase expressing macrophages has been described in tumors, and these cells have been shown to inhibit CD8 T-cell responses (40). We purified $CD11b^+Gr1^{hi}$ and $CD11b^+Gr1^{lo}$ cells from tumors by FACS and tested for arginase expression by Western blot and enzyme assay. In agreement with the results of Rodriguez and colleagues (40), predominant arginase protein expression and enzyme activity was found in the $CD11b^+Gr1^{lo}$ mature macrophage population (data not shown).

To test the function of the different macrophage populations in tumors, we purified $CD11b^+Gr1^{hi}$ and $CD11b^+Gr1^{lo}$ cells from tumors by FACS sorting. These cells were tested for their ability to inhibit proliferation of CFSE-labeled CD8 T cells *in vitro*. Interestingly, whereas $CD11b^+Gr1^{lo}$ cells purified from control tumors greatly inhibited CD8 T-cell proliferation, this same population purified from tumors in animals treated with aOX40 were much less inhibitory. The MDSC phenotype tumor $CD11b^+Gr1^{hi}$ cells from either control-treated or aOX40-treated animals were not inhibitory in this *in vitro* assay. These data strongly suggest that mature macrophages in the tumor environment suppress CD8 T-cell responses. Systemic OX40 therapy changes the tumor environment and the function of the $CD11b^+Gr1^{lo}$ cells to make a significantly less suppressive environment.

Discussion

The experiments reported here show that systemic administration of αOX40 results in profound changes in the immune status of

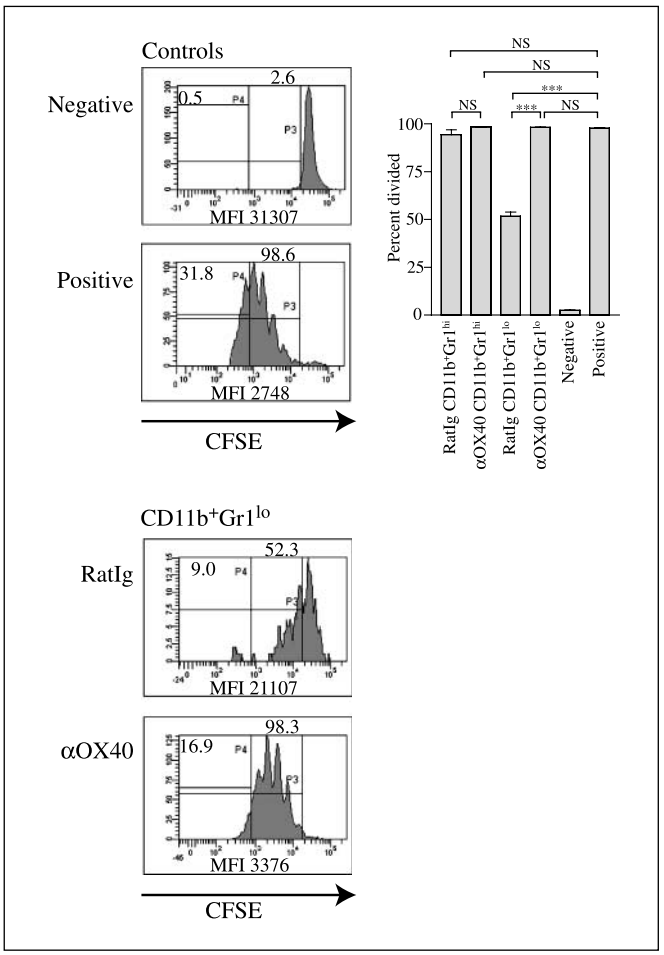

Figure 6. Function of tumor-infiltrating macrophage populations in T-cell proliferation assays and the effect of αOX40. $CD11b^+Gr1^{hi}$ and $CD11b^+Gr1^{lo}$ cells were purified from MCA205 H12 tumors grown in C57BL/6 mice 7 d after treatment with control RatIg or αOX40. 5×10^4 $CD11b^+Gr1^{hi}$ or $CD11b^+Gr1^{lo}$ cells were combined with 5×10^4 $CFSE^+$–labeled $CD8^+$ cells from control spleens along with CD3-depleted spleen cells as accessory cells and 1 μg/mL αCD3. Histograms show CFSE dilution in representative samples 96 h after initiation of the culture. *Columns,* percentage of CD8 divided from triplicate samples. *, $P < 0.05$; **, $P < 0.01$; ***, $P < 0.001$.

the tumor environment. These changes included significant increases in the percentage of CD8 T cells at the tumor site (Fig. 1), with differentiation toward an effector phenotype and evidence of increased function (Fig. 2). αOX40 therapy also significantly increased the proportion of tumor-associated antigen-specific CD8 T cells at the tumor site, which required direct interaction of αOX40 upon the antigen-specific CD8 T cells (Fig. 2). While tumor-infiltrating T regulatory cells expressed OX40 and there was a decrease in the proportion of CD4 T cells that were T regulatory phenotype after αOX40 therapy (Fig. 3), the function of T regulatory cells was not altered after systemic αOX40 therapy (Fig. 3). These data diminish the likelihood that alteration in T regulatory cell function was responsible for the influx of CD8 T cells into the tumors of αOX40-treated mice. αOX40 therapy also changed the tumor stromal cells, causing a decline in both macrophages and MDSC (Fig. 4). This effect was independent of CD4 cells, but dependent on CD8 T cells (Fig. 5). We found that the tumor-infiltrating cells from αOX40-treated mice expressed lower levels of TGFβ mRNA, although the decrease may be due solely to the reduced proportion of T regulatory cells and macrophages within the tumor site (Fig. 5). Finally, we showed that the mature macrophages purified from the tumor site greatly inhibited CD8 T-cell responses. Systemic treatment with aOX40 altered the function of these cells, resulting in significantly less T-cell suppression (Fig. 6).

These data suggest that αOX40 induced a shift in the immune environment of the tumor. It has been widely reported that the tumor is a relatively immunosuppressed environment (15, 41), with infiltration by T regulatory cells (21, 22), suppressive macrophages (42, 43), and production of inhibitory cytokines (38, 44). Impressively, αOX40 therapy clearly influenced several of these factors and seemed to do so primarily via enhanced infiltration of tumors by tumor-specific CD8 cells. The access of effector cells to the tumor is of critical importance to the success of immunotherapy for solid tumors. In contrast to models of metastasis, the presence of large numbers of activated tumor-specific effector CD8 T cells does not necessarily correlate with efficacy in solid primary tumors. *In vivo* experiments have shown limited tumor-specific trafficking of adoptively transferred tumor-specific T cells (45). Thus, modification of the tumor site to attract T cells can increase the efficacy of adoptive T-cell therapies (31), but such therapies require knowledge of or access to the tumor site. This issue underscores the importance of the finding that a systemically delivered αOX40 antibody caused an increase in tumor-specific CD8 T cells at the tumor site. That this effect occurred with endogenous effector cells is extremely valuable, because it does not require labor-intensive techniques to generate tumor-specific T cells or limit therapy to those patients or cancers with known MHC or antigen status. We show here very similar effects in models of sarcoma, mammary carcinoma, and colorectal carcinoma in two different strains of laboratory mice, suggesting broad applicability.

Previous work from our laboratory showed that infusion of OX40 agonists into tumor-bearing hosts resulted in increased tumor-free survival in a variety of tumor models (19, 20, 46). The agonists were delivered early after tumor challenge, and the effects were lost if either CD4 or CD8 T cells were depleted during the priming or effector phases (20, 46). The experiments described here occur at times beyond early tumor priming, such that the tumor-bearing animals may already have developed functional effector T cells, albeit within a suppressive environment (47, 48). Thus, in these experiments, there was a lesser requirement for CD4 T cells in the response and more of a requirement to overcome CD8 tolerogenic mechanisms. Importantly, it has recently been shown that treatment with agonist antibodies to OX40 can overcome CD8 anergy (49). This may also distinguish our results from those of Song and colleagues, where agonistic OX40 antibodies increased peritoneal accumulation of antigen-specific CD8 T cells (11, 50), but the effectiveness was dependent on ligation of OX40 on CD4, not CD8 T cells (50). In their experiments, CD4 depletion was performed before tumor challenge; thus, there was no CD4 help during initial CD8 priming, most likely resulting in defective CD8 immunity. In our model, where an initial endogenous immune response can develop in the presence of CD4 T cells, αOX40 activity may be more important to overcome subsequent CD8 anergy rather than *de novo* priming. The mechanism by which this occurs remains to be determined. Although we show that antigen-specific CD8 T cells must express OX40 to accumulate in the tumor after OX40 therapy, they exist in a draining lymph node environment that is also responding to the tumor and the OX40 therapy. Thus, the

precise interaction between CD4 and CD8 T cells in the established tumor remains to be determined. One possibility is simply improved survival of the OT1 cells. Alternatively, recent data from our laboratory show that OX40 ligation on CD8 T cells directly influences their maturation into full effector cells (51). Notably, we showed the diminished presence of macrophages at the tumor site, loss or maturation of the immature MDSC population, and decreased TGFβ mRNA. These changes fit very well with our data showing the time course of T-cell accumulation in the tumor and support the hypothesis that the initial actions of OX40 therapy is on T cells that has secondary consequences to the tumor environment. Thus, we propose that one mechanism by which OX40 ligation on CD8 T cells enhances immune clearance of established tumors is through these secondary changes that occur within the tumor environment, potentially providing a therapeutic window for effective antitumor immunity. In this way, decreased MDSC or decreased cells secreting TGFβ may feedback to decrease differentiation of T regulatory cells (27) or permit further accumulation of CD8 T cells (38).

However, a single administration of αOX40 may not be able to sustain this positive environment. In the absence of further adjuvant activity and in the face of continued tumor growth and secretion of factors, such as TGFβ, it is reasonable to expect reestablishment of suppressive macrophage and T regulatory cell dominance and subsequent CD8 T cell anergy or deletion. Further studies will examine the effect of repeated αOX40 dosing of mice with established tumors and the long-term consequences on the tumor immune environment. Nevertheless, systemic treatment with agonist OX40 antibodies provides critical signals for immune reactivation without prior knowledge of tumor or immune specificity and an opportunity for therapeutic intervention.

Disclosure of Potential Conflicts of Interest

No potential conflicts of interest were disclosed.

Acknowledgments

Received 12/3/2007; revised 4/7/2008; accepted 4/24/2008.

Grant support: NIH grant R01 CA102577 and medical research grants from the Miller Foundation and M.J. Murdock Charitable Trust.

The costs of publication of this article were defrayed in part by the payment of page charges. This article must therefore be hereby marked *advertisement* in accordance with 18 U.S.C. Section 1734 solely to indicate this fact.

We thank Daniel Haley for assistance in flow cytometry analysis and sorting and Dr. Walter Urba for excellent comments and advice on the manuscript.

References

1. Evans DE, Prell RA, Thalhofer CJ, Hurwitz AA, Weinberg AD. Engagement of OX40 enhances antigen-specific CD4(+) T cell mobilization/memory development and humoral immunity: comparison of αOX-40 with αCTLA-4. J Immunol 2001;167:6804–11.

2. Maxwell JR, Weinberg A, Prell RA, Vella AT. Danger and OX40 receptor signaling synergize to enhance memory T cell survival by inhibiting peripheral deletion. J Immunol 2000;164:107–12.

3. Gramaglia I, Jember A, Pippig SD, Weinberg AD, Killeen N, Croft M. The OX40 costimulatory receptor determines the development of CD4 memory by regulating primary clonal expansion. J Immunol 2000; 165:3043–50.

4. Weatherill AR, Maxwell JR, Takahashi C, Weinberg AD, Vella AT. OX40 ligation enhances cell cycle turnover of Ag-activated CD4 T cells *in vivo*. Cell Immunol 2001;209: 63–75.

5. Ohshima Y, Tanaka Y, Tozawa H, Takahashi Y, Maliszewski C, Delespesse G. Expression and function of OX40 ligand on human dendritic cells. J Immunol 1997;159:3838–48.

6. Kopf M, Ruedl C, Schmitz N, et al. OX40-deficient mice are defective in Th cell proliferation but are competent in generating B cell and CTL responses after virus infection. Immunity 1999;11:699–708.

7. Croft M, Duncan DD, Swain SL. Response of naive antigen-specific CD4+ T cells *in vitro*: characteristics and antigen-presenting cell requirements. J Exp Med 1992;176:1431–7.

8. Ruby CE, Redmond WL, Haley D, Weinberg AD. Anti-OX40 stimulation *in vivo* enhances CD8+ memory T cell survival and significantly increases recall responses. Eur J Immunol 2007;37:157–66.

9. Lee SW, Park Y, Song A, Cheroutre H, Kwon BS, Croft M. Functional dichotomy between OX40 and 4-1BB in modulating effector CD8 T cell responses. J Immunol 2006;177:4464–72.

10. Fujita T, Ukyo N, Hori T, Uchiyama T. Functional characterization of OX40 expressed on human CD8+ T cells. Immunol Lett 2006;106:27–33.

11. Song A, Tang X, Harms KM, Croft M. OX40 and Bcl-xL promote the persistence of CD8 T cells to recall tumor-associated antigen. J Immunol 2005;175:3534–41.

12. Marzo AL, Lake RA, Lo D, et al. Tumor antigens are constitutively presented in the draining lymph nodes. J Immunol 1999;162:5838–45.

13. Kawakami Y, Eliyahu S, Delgado CH, et al. Cloning of the gene coding for a shared human melanoma antigen recognized by autologous T cells infiltrating into tumor. Proc Natl Acad Sci U S A 1994;91:3515–9.

14. Robbins PF, el-Gamil M, Li YF, et al. Cloning of a new gene encoding an antigen recognized by melanoma-specific HLA-A24-restricted tumor-infiltrating lymphocytes. J Immunol 1995;154:5944–50.

15. Luscher U, Filgueira L, Juretic A, et al. The pattern of cytokine gene expression in freshly excised human metastatic melanoma suggests a state of reversible anergy of tumor-infiltrating lymphocytes. Int J Cancer 1994;57:612–9.

16. Walker EB, Haley D, Miller W, et al. gp100(209–2M) peptide immunization of human lymphocyte antigen-A2+ stage I-III melanoma patients induces significant increase in antigen-specific effector and long-term memory CD8+ T cells. Clin Cancer Res 2004;10:668–80.

17. Yoshioka T, Nakajima A, Akiba H, et al. Contribution of OX40/OX40 ligand interaction to the pathogenesis of rheumatoid arthritis. Eur J Immunol 2000;30: 2815–23.

18. Weinberg AD, Wegmann KW, Funatake C, Whitham RH. Blocking OX-40/OX-40 ligand interaction *in vitro* and *in vivo* leads to decreased T cell function and amelioration of experimental allergic encephalomyelitis. J Immunol 1999;162:1818–26.

19. Morris A, Vetto JT, Ramstad T, et al. Induction of anti-mammary cancer immunity by engaging the OX-40 receptor *in vivo*. Breast Cancer Res Treat 2001;67:71–80.

20. Weinberg AD, Rivera MM, Prell R, et al. Engagement of the OX-40 receptor *in vivo* enhances antitumor immunity. J Immunol 2000;164:2160–9.

21. Curiel TJ, Coukos G, Zou L, et al. Specific recruitment of regulatory T cells in ovarian carcinoma fosters immune privilege and predicts reduced survival. Nat Med 2004;10:942–9.

22. Sato E, Olson SH, Ahn J, et al. Intraepithelial CD8+ tumor-infiltrating lymphocytes and a high CD8+/regulatory T cell ratio are associated with favorable prognosis in ovarian cancer. Proc Natl Acad Sci U S A 2005;102:18538–43.

23. Awwad M, North RJ. Immunologically mediated regression of a murine lymphoma after treatment with anti-L3T4 antibody. A consequence of removing L3T4+ suppressor T cells from a host generating predominantly Lyt-2+ T cell-mediated immunity. J Exp Med 1988;168: 2193–206.

24. Shimizu J, Yamazaki S, Sakaguchi S. Induction of tumor immunity by removing CD25+CD4+ T cells: a common basis between tumor immunity and autoimmunity. J Immunol 1999;163:5211–8.

25. Takeda I, Ine S, Killeen N, et al. Distinct roles for the OX40–40 ligand interaction in regulatory and non-regulatory T cells. J Immunol 2004;172:3580–9.

26. Valzasina B, Guiducci C, Dislich H, Killeen N, Weinberg AD, Colombo MP. Triggering of OX40 (CD134) on CD4(+)CD25+ T cells blocks their inhibitory activity: a novel regulatory role for OX40 and its comparison with GITR. Blood 2005;105:2845–51.

27. Vu MD, Xiao X, Gao W, et al. OX40 costimulation turns off Foxp3+ Tregs. Blood 2007;110:2501–10.

28. Hogquist KA, Jameson SC, Heath WR, Howard JL, Bevan MJ, Carbone FR. T cell receptor antagonist peptides induce positive selection. Cell 1994;76:17–27.

29. Pippig SD, Pena-Rossi C, Long J, et al. Robust B cell immunity but impaired T cell proliferation in the absence of CD134 (OX40). J Immunol 1999;163:6520–9.

30. Wang G, Savinko T, Wolff H, et al. Repeated epicutaneous exposures to ovalbumin progressively induce atopic dermatitis-like skin lesions in mice. Clin Exp Allergy 2007;37:151–61.

31. Gough M, Crittenden M, Thanarajasingam U, et al. Gene therapy to manipulate effector T cell trafficking to tumors for immunotherapy. J Immunol 2005;174: 5766–73.

32. Kim CH, Kunkel EJ, Boisvert J, et al. Bonzo/CXCR6 expression defines type 1-polarized T-cell subsets with extralymphoid tissue homing potential. J Clin Invest 2001;107:595–601.

33. Sato T, Thorlacius H, Johnston B, et al. Role for CXCR6 in recruitment of activated CD8+ lymphocytes to inflamed liver. J Immunol 2005;174:277–83.

34. Bronte V, Apolloni E, Cabrelle A, et al. Identification of a CD11b(+)/Gr-1(+)/CD31(+) myeloid progenitor capable of activating or suppressing CD8(+) T cells. Blood 2000;96:3838–46.

35. Kusmartsev SA, Li Y, Chen SH. Gr-1+ myeloid cells derived from tumor-bearing mice inhibit primary T cell activation induced through CD3/CD28 costimulation. J Immunol 2000;165:779–85.

36. Ghiringhelli F, Menard C, Terme M, et al. CD4+CD25+ regulatory T cells inhibit natural killer cell functions in a transforming growth factor-β-dependent manner. J Exp Med 2005;202:1075–85.

37. Huang B, Pan PY, Li Q, et al. Gr-1+CD115+ immature myeloid suppressor cells mediate the development of

tumor-induced T regulatory cells and T-cell anergy in tumor-bearing host. Cancer Res 2006;66:1123–31.
38. Zhang Q, Yang X, Pins M, et al. Adoptive transfer of tumor-reactive transforming growth factor-β-insensitive CD8+ T cells: eradication of autologous mouse prostate cancer. Cancer Res 2005;65:1761–9.
39. Bronte V, Zanovello P. Regulation of immune responses by L-arginine metabolism. Nat Rev Immunol 2005;5:641–54.
40. Rodriguez PC, Quiceno DG, Zabaleta J, et al. Arginase I production in the tumor microenvironment by mature myeloid cells inhibits T-cell receptor expression and antigen-specific T-cell responses. Cancer Res 2004;64:5839–49.
41. Whiteside TL. Signaling defects in T lymphocytes of patients with malignancy. Cancer Immunol Immunother 1999;48:346–52.
42. Young MR, Wright MA, Lozano Y, et al. Increased recurrence and metastasis in patients whose primary head and neck squamous cell carcinomas secreted granulocyte-macrophage colony-stimulating factor and contained CD34+ natural suppressor cells. Int J Cancer 1997;74:69–74.
43. Almand B, Clark JI, Nikitina E, et al. Increased production of immature myeloid cells in cancer patients: a mechanism of immunosuppression in cancer. J Immunol 2001;166:678–89.
44. Coussens LM, Werb Z. Inflammation and cancer. Nature 2002;420:860–7.
45. Griffith KD, Read EJ, Carrasquillo JA, et al. *In vivo* distribution of adoptively transferred indium-111-labeled tumor infiltrating lymphocytes and peripheral blood lymphocytes in patients with metastatic melanoma. J Natl Cancer Inst 1989;81:1709–17.
46. Kjaergaard J, Peng L, Cohen PA, Drazba JA, Weinberg AD, Shu S. Augmentation versus inhibition: effects of conjunctional OX-40 receptor monoclonal antibody and IL-2 treatment on adoptive immunotherapy of advanced tumor. J Immunol 2001;167:6669–77.
47. Bursuker I, North RJ. Generation and decay of the immune response to a progressive fibrosarcoma. II. Failure to demonstrate postexcision immunity after the onset of T cell-mediated suppression of immunity. J Exp Med 1984;159:1312–21.
48. North RJ, Bursuker I. Generation and decay of the immune response to a progressive fibrosarcoma. I. Ly-1+2- suppressor T cells down-regulate the generation of Ly-1–2+ effector T cells. J Exp Med 1984;159:1295–311.
49. Murata S, Ladle BH, Kim PS, et al. OX40 costimulation synergizes with GM-CSF whole-cell vaccination to overcome established CD8+ T cell tolerance to an endogenous tumor antigen. J Immunol 2006;176:974–83.
50. Song A, Song J, Tang X, Croft M. Cooperation between CD4 and CD8 T cells for anti-tumor activity is enhanced by OX40 signals. Eur J Immunol 2007;37:1224–32.
51. Redmond WL, Gough MJ, Charbonneau B, Ratliff TL, Weinberg AD. Defects in the acquisition of CD8 T cell effector function after priming with tumor or soluble antigen can be overcome by the addition of an OX40 agonist. J Immunol 2007;179:7244–53.